



ELSEVIER



Review Article

Simulations employing finite element method at liquid|liquid interfaces

Pekka Peljo^{1,*}, Micheál D. Scanlon² and T. Jane Stockmann^{3,*}

Simulated curves compared to recorded data have provided a breadth of insight into mechanisms and kinetic aspects of charge transfer at the liquid|liquid interface (LLI). This is often performed with software employing finite element methods (FEMs). The advent and application of this asset to soft interfacial chemistry has allowed a more facile exploration of geometric considerations, the role of interfacial size (from macro to nano), while simultaneously expanding to include homo/heterogeneous reactions such as electrocatalytic, photochemical, nanoparticle interactions, etc. This article provides insight into the status of the field of LLI FEM studies as well as a perspective as to what role simulations and numerical analysis will play in the future.

Addresses

¹ Laboratoire d'Electrochimie Physique et Analytique, École Polytechnique Fédérale de Lausanne (EPFL Valais Wallis), Rue de l'Industrie, 17, 1951, Sion, Switzerland

² The Bernal Institute and Department of Chemical Sciences, School of Natural Sciences, University of Limerick (UL), Limerick V94 T9PX, Ireland

³ Sorbonne Paris Cité, Paris Diderot University, Interfaces, Traitements, Organisation et Dynamique des Systèmes, CNRS-UMR 7086, 15 rue J.A. Baïf, Paris 75013, France

*Corresponding authors: Peljo, Pekka (pekka.peljo@epfl.ch), Stockmann, T. Jane (jane.stockmann@univ-paris-diderot.fr)

To facilitate this, the geometry is subdivided by a mesh consisting of elements, e.g. free triangular or quadrilateral. In this *discretization*, the problem is then solved for each element and subsequently compared to the whole. FEM has been an invaluable utility for electrochemists in battery, materials, mass transport problems, etc. and has been comprehensively reviewed [1–3]. More complex simulations of electrochemical systems, for example by molecular dynamics or by density functional theory, are outside the scope of this article.

Electrochemistry at interfaces between two immiscible electrolyte solutions (ITIES) is a distinct and versatile area of contemporary electrochemistry, as summarized by recent reviews [4–9]. This review will focus on digital simulations of electrochemical processes at ITIES, highlighting the applications as well as the perspectives. [Scheme 1](#) illustrates the development of a simulation from the experiment, in this case an interface held at the tip of a pipette – a micro-ITIES, as well as mesh refinement. Refining the mesh can be a particularly challenging aspect of the FEM; too fine and run-times become prohibitively long, too coarse and the result is not accurate or precise. Great care should be given to this step, with comparison using simple mechanics to known analytical solutions before moving forward with more exotic systems.

Current Opinion in Electrochemistry 2017, 7:200–207

This review comes from a themed issue on **Fundamentals LYONS**

Edited by **Mike Lyons**

For a complete overview see the [Issue](#) and the [Editorial](#)

Available online 27 September 2017

<https://doi.org/10.1016/j.coelec.2017.09.011>

2451-9103/© 2017 Elsevier B.V. This is an open access article under the CC BY license. (<http://creativecommons.org/licenses/by/4.0/>)

Charge transfer simulations at an ITIES

While conventional electrochemistry operates at a solid|liquid interface, e.g. metal (Pt, Au, etc.) or carbon, fundamentally analogous charge transfer reactions can take place at LLIs such as water|oil (w|o), or even w|ionic liquid (w|IL). This means that the same electrochemical techniques (e.g., cyclic voltammetry (CV)) and theory of charge transfer can be transposed to so-called soft interfaces. This is advantageous as LLI electrochemistry is not limited to redox electrochemistry, but also includes simple and facilitated ion transfer (FIT) reactions, where ions are pushed or pulled across an interface. Simple ion transfer (IT) of ion *i* with charge *z* transferring from water (w) to oil (o) is given through the following reaction:

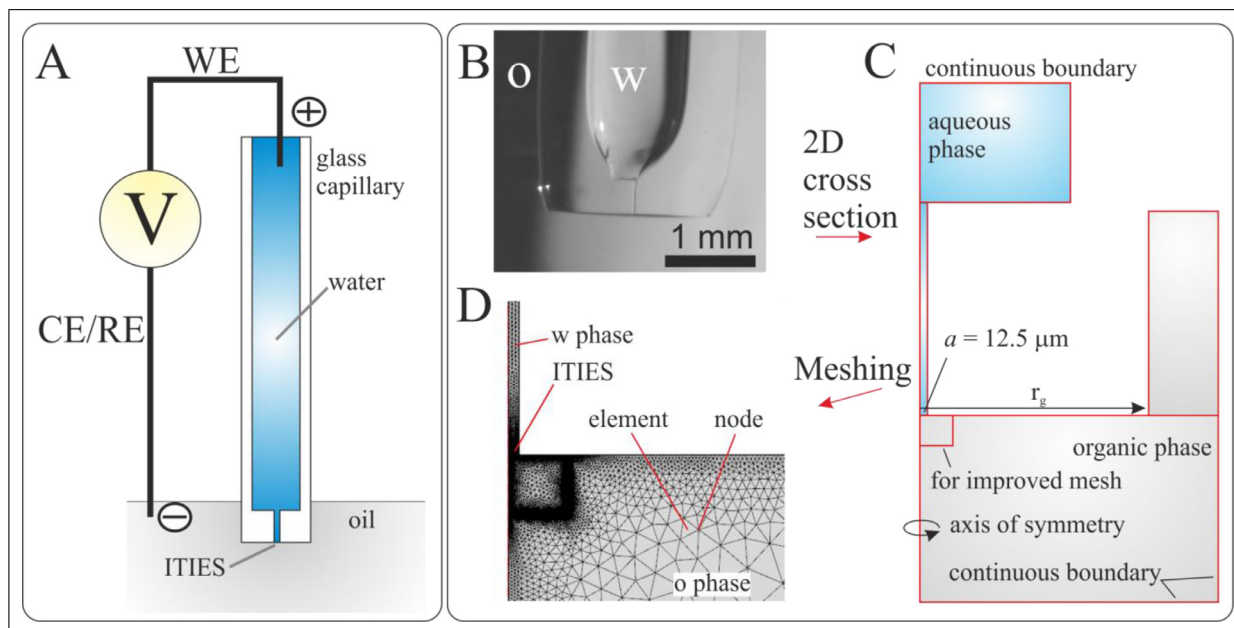


Ions are manipulated by biasing the potential across the ITIES using electrodes immersed in either phase. The potential drop is localized across the w|o interface (~1 nm) and called the Galvani potential difference ($\phi_w - \phi_o = \Delta_o^w \phi$); where ϕ_w and ϕ_o are the potentials in

Introduction

Finite element method (FEM) simulation software is ultimately a synthesis of established analytical equations with geometric components. These can then contain complex material properties or be combined with multiple physics (so-called multi-physics), or equation sets, e.g. heat transfer with electrical conduction. The degree of complexity of these systems necessitates their numeri-

Scheme 1



(A) schematic of a micropipette ITIES experimental setup; (B) photograph of the pipette tip immersed in an organic phase (o) with an aqueous (w) solution held inside and the interface at the tip; (C) the pipette tip converted to 2D axial symmetric geometry, taking advantage of the infinite rotational symmetry C_{∞} element of the cylindrical capillary and further reducing it in half greatly reduces the computational effort and simulation run time; (D) illustrates the mesh surrounding the simulated ITIES shown in C, where an additional geometry element, a box, has been added to better refine the mesh in the area of hemispherical diffusion in the vicinity of the ITIES on the o side.

phase w and o , respectively. $\Delta_o^w \phi$ is controlled via electrodes positioned in either phase. In this way, $\Delta_o^w \phi$ is similar to E or the potential drop across a solid|liquid boundary and the kinetics of IT are often handled using a Butler–Volmer model [4]. These equations often form the basis for most simulations, which can then be expanded upon for further complexity. Indeed, the driver for digital simulations is often the absence of a simplified analytical solution.

Fundamental studies

Droplet or thick-film modified electrodes are one macro-ITIES (mm^2 to cm^2) system often simulated, with electron transfer (ET) across the electrode-droplet interface coupled to IT across the LLI. Zanotto *et al.* [10[•]] recently explored a solid electrode completely covered by a thick organic film, which was then immersed in an aqueous phase, using a 1D simulation. They showed [10[•]] that the coupled effect of ET at the solid| o interface with IT at $w|o$ had an appreciable influence on the shape, peak-to-peak potential difference, as well as the mid-peak potential in the i - V curve. The numerical simulations could satisfactorily explain deviation from the 59 mV peak-to-peak separation expected for a reversible ET or IT reaction (number of electrons $z = 1$ for ET or singly charged species for IT). This approach is actually similar to typical ionophore-based ion-selective electrodes (ISE) [11], where a solid conducting polymer is used for ET that is coupled with

transfer of an analyte ion across the water-membrane interface. Simulations of these kinds have been considered by Lewenstam utilizing Nernst–Planck–Poisson equations [12], and by Amemiya [13,14] and Bakker's groups [15[•],16] for the fully electrolyte supported case; i.e. Fick's laws of diffusion.

These simulations were extended to 2D to study coupled ET–IT reactions upon collision of organic droplets with an electrode [17[•]], considering both diffusion and migration. In this case, the secondary or tertiary current distribution was also solved to show that the iR drop in the toluene solution is negligible. Furthermore, both the entire electrode| o and $w|o$ surface are electrochemically active, despite higher current densities at the three-phase boundary. From comparison with the experimental data, it was apparent that the colliding droplets had quite high contact angles with the electrode after collision.

Meanwhile, the exact mechanism of ET across LLIs has been a subject of controversy [2]. This topic was recently revisited by a combination of experiments and FEM simulations of ET between ferrocene (Fc) and hexacyanoferrate (FeCN_6^{4-}) [18[•]]. Comparison with experimental and simulated CVs indicate that the likely mechanism is one of potential independent Fc partitioning to w with subsequent Fc oxidation/ FeCN_6^{4-} reduction in the bulk aqueous phase, followed by potential-dependent Fc^+

transfer back from $w \rightarrow o$. These data agree well with the earlier experimental and simulated results of Osakai and co-workers [19]. If a gold nanofilm was added to the interface, it behaved as a bipolar electrode and electrons were shuttled through the gold film in a heterogeneous interfacial redox electrocatalysis [18[•],20]. Stockmann *et al.* [21[•]] exploited the Pt nanoparticle catalysis of O₂ reduction at a LLI for single nanoparticle impact studies; whereby, as a nanoparticle impacts with the interface a spike from the electrocatalytically enhanced reaction is recorded in the current transient in the pA range. Nanoparticle simulations [21[•]] at the LLI were used to explore the effect of penetration depth, through a symmetrically bifurcated sphere cap and superhemisphere, on the spike current intensity. These simulations also confirmed the necessity of an O₂ partitioning mechanism – between water and 1,2-dichloroethane – proposed by Trojáněk *et al.* [22].

1D simulations have provided insight into differential capacitance at the back-to-back double layers formed when a LLI is established. These showed that the width and symmetry of the two interfacial regions are crucial parameters and experimental capacitance data could be used to estimate the width of the interfacial region, which the authors suggest is on the order of 3 nm [23]. FEM was also used to calculate the current distribution in a large rectangular cell with smaller electrodes, ruling out the current distribution as an explanation for the driving force for a Marangoni shutter where gold nanoparticles, adsorbed at the ITIES, move to the center of the cell and to the edges as a function of the applied polarization [24].

Additionally, FEM have been utilized for detailed characterization of a flexible thin layer electrochemical flow cell for ultrasensitive amperometric detection at an ITIES, reaching nanomolar detection limits [25]. If ITIES-based devices become more common, this kind of simulation will be extremely useful for device optimization. The recent use of macro scale (mm→cm) models [10[•],16,18[•],26[•]–29] suggests that there is a thriving field of study for bulk material properties, their interaction with the LLI, and the fundamental interrogation of the LLI's physical properties.

With the rapid development of modern micro [30,31], and nano fabrication techniques [32,33], there was a push toward miniaturization owing to a number of benefits. These included reduced capacitance/solution resistance due to the lower operational current range and thus, no longer required *i*R-compensation. This meant that the interfacial surface (e.g. radius of a disc interface) was smaller than the diffusion layer thickness ($\delta \approx (Dt)^{1/2}$) at most scan rates and hence steady state current profiles were generated. This improved mass transport increased the experimental sensitivity permitting the exploration of faster charge transfer reactions and had a concomitant increased

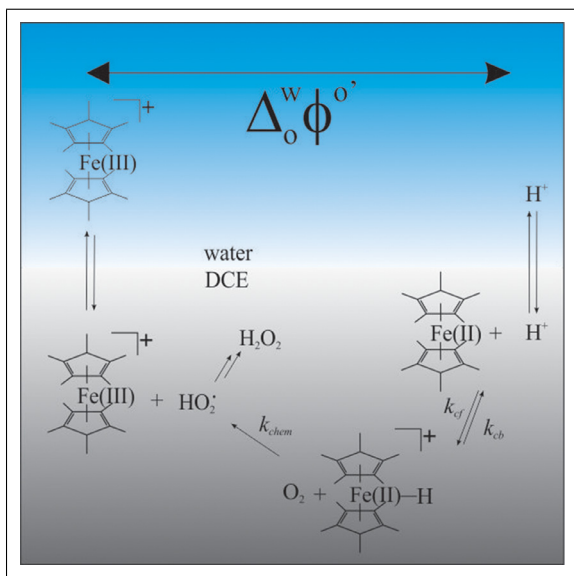
interest toward their characterization through simulation. A recent perspective by Arrigan and Herzog [8[•]] in this journal examined simple IT and so the concept is only briefly introduced here. Additionally, electrochemistry at macro, micro, and nano interfaces has been reviewed recently [7,9]. One of the first simulations by Girault's group [34] focused on the position of the LLI at a micropore; on either side or within a microchannel. Later, pore angle and spacing were explored for micro-ITIES arrays by Arrigan's group [35,36]. This was extended to interfaces housed at the tip of pulled borosilicate or quartz glass capillaries [37,38]. Nishi *et al.* [37] examined the geometric effect combined with a viscous secondary phase, specifically w|IL vs. w|o interfaces, where the diffusion coefficient is 3–4 orders of magnitude lower for the former vs. the latter. This causes the *i*-V profile to resemble a macro-ITIES signal with linear diffusion dominating in both IT directions owing to the increased viscosity in the IL phase, whereas w diffusion is confined by the pipette walls. In 2009, Rodgers *et al.* [38] examined the effect of taper angle on pulled quartz pipettes, the diffusion of species, and the resultant *i*-V signal. They demonstrated that forward and reverse waves could characterize the geometric and transport properties of the pulled pipette [38] with a high degree of sensitivity. Simultaneously, micro LLI arrays have been developed and explored, e.g. Alvarez de Eulate *et al.* [39], with the goal of understanding interface location and its impact on *i*-V curves.

The complexity of these models was increased to examine FIT processes with typically 3–4 processes being considered [5]. This has led to studies at the $w|IL$ interface [40] where ILs have been shown to be excellent solvents for metal ion extraction, but also the utility of somewhat exotic organic solvents, like CHCl₃ [41]. In the latter [41], a phospholipid, 1,2-dimyristoyl-sn-glycero-3-phosphocholine (DMPC), highly soluble in CHCl₃ ($\epsilon = 4.81$), was investigated at a blunt pulled micro-ITIES ($\varnothing = 25 \mu\text{m}$). This confirmed that the analytical solution of FIT, formulated for a macro-ITIES, was transposable to the micro-ITIES platform employed.

Electrocatalytic reactions

Owing to its biomimetic nature, there are a number of valuable electrocatalytic reactions such as the O₂ reduction reaction (ORR) that are of considerable interest. This is exemplified through the recent work by Girault's group [26–28], examined through a macro-ITIES 1D simulation. Therein, Girault and co-workers examined the ORR (see Figure 1) using decamethylferrocene (DMFc), and other metallocenes as catalyst/electron donor in the oil phase and H₂SO₄ as the proton source in the aqueous phase. Protons are pushed across the interface at high positive potentials and coordinate with DMFc in the bulk oil phase in the vicinity of the ITIES. While the DMFc hydride formation, and subsequent oxidation, were treated as bulk processes, the speed of the reaction in-

Figure 1



Mechanism of O_2 reduction using decamethylferrocene as both electron donor and catalyst, while the liquid|liquid interface, between water|1,2-dichloroethane (w|DCE) acts as the junction for charge separation.

Source: Adapted from Journal of Electroanalytical Chemistry, Vol 729, Stockmann T.J, Deng H, Peljo P, Kontturi K, Opallo M, Girault H.H, Mechanism of oxygen reduction by metallocenes near liquid|liquid interfaces, Pages No.43-52, Copyright 2014, with permission from Elsevier [27].

indicated that the reaction layer was small, $\sim 50 \mu\text{m}$, compared to the diffusion layer thickness without O_2 reduction, $\sim 200 \mu\text{m}$ [27]. Simulated and experimental CVs were compared through two curve features: (i) the absence of a proton return peak in the edge-of-scan profile and (ii) the $DMFc^+$ transfer peak intensity. Through a similar process, this group examined the surprising O_2 reduction at LLIs in the presence of alkali metals or rather their hydration sphere, whose protons are made acidic as they transfer across the ITIES [28,29].

Optimizing or predicting the reaction layer thickness of a system is a valuable utility when trying to incorporate additional *in situ* detection methods to complement the electrochemical ones, such as electrogenerated chemiluminescence, scanning electrochemical microscopy (SECM), etc.

SECM simulations

SECM digital simulations have been utilized extensively for LLIs. For example, H_2O_2 generated from O_2 reduction by DMFc at a trifluorotoluene|water (TFT|w) interface was probed by a SECM tip sensitive to H_2O_2 , and the experimental results were compared with FEM simulated curves. If the H_2O_2 generation was modeled as a constant flux from the ITIES, simulations show negative feedback

close to the interface, while the experiments show continuous increase also close to the interface. Hence, a model considering H_2O_2 generation within the $50 \mu\text{m}$ thick uniform reaction zone was considered to obtain better agreement with the experimental data [42].

Mirkin and co-workers proposed ET/IT as a new mode of SECM operation, using a nanometer sized pipette filled with an organic phase containing a neutral redox mediator [43]. This redox mediator can partition into the aqueous phase and undergo redox reactions at the substrate. The ions produced in this ET reaction can be transferred into the organic filling solution of the nanopipette in an IT reaction, giving rise to a measurable IT tip current. Transfer of other ions at the tip can be used for distance control in negative feedback mode. Digital simulations were employed to study the ET/IT feedback considering (i) the partitioning of neutral redox species from the pipette to the external solution, (ii) diffusion of these species to and their oxidation (or reduction) at the conductive substrate, (iii) diffusion of the reaction product to the pipette orifice, and (iv) IT at the tip ITIES. This approach was later used to detect short-lived intermediates of electrocatalytic O_2 reduction, by using O_2 as a redox mediator for the ET reaction, and measuring the IT current of the O_2^- intermediate [44]. Additionally, simulations can be used to generate analytical approximations, as done recently by Oleinick *et al.* [45] for the ET/IT SECM configuration where the surface-generated ionic species is either chemically stable or participates in a first- or second-order homogeneous reaction.

Furthermore, digital simulations of SECM have been used to study the kinetics of O_2 reduction by DMFc in acidified DCE in an EC' mechanism, where DMFc generated at the SECM tip reacted homogeneously with O_2 and protons to regenerate the initial $DMFc^+$. Through comparison of simulated and experimental curves an apparent rate constant for the homogeneous reaction was obtained [46].

Nanopores fabricated in a nanocrystalline silicon membrane have been probed by SECM with a high degree of resolution achieved through the use of a nanopipette [47,48]. FEM simulation was employed to investigate the spatial resolution of the approach [47]. This report has interesting implications toward biological cellular imaging particularly when combined with the following: (i) the recent work by Kuss *et al.* [49] that used high speed SECM imaging with a Pt disc micro electrode in conjunction with a forced convection numerical model to study the redox properties of live cells; (ii) as well as the work of Henderson *et al.* [50] in the development of a 3D topographical simulation for their live cell investigations. The combination of these three works suggests one direction SECM and numerical analysis could take. That is, rapid bio-imaging of cells using liquid|liquid junction scanning

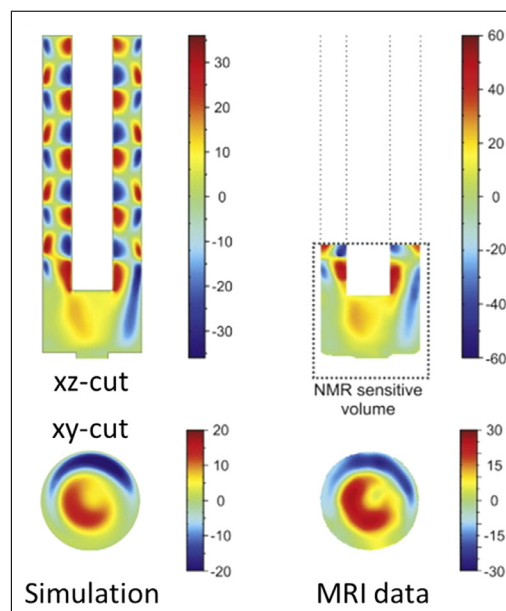
probes with a high degree of spatial resolution. With this, a more comprehensive picture of bio-cellular processes could be gained in conjunction with the simultaneous response of live cells to external stimuli. The LLI offers the possibility to investigate living cells using non-redox active charged species. This is demonstrative of one potential avenue for FEM simulation development and application.

Multiphysics approach

Ovejero *et al.* have studied the effect of forced hydrodynamic convection on both IT and FIT, both theoretically and experimentally [51]. This is an example of a typical approach where the fluid velocity was assumed independent of the distance from the stirrer [51]. This assumption is reasonable if the electrode distance from the stirrer is large enough, reaching a constant value of $0.88447 \times \sqrt{\nu\omega}$, where ν is the kinematic viscosity and ω is the angular velocity of rotation, as demonstrated by Levich [52]. Additionally, hydrodynamic conditions produced by the rotating stirrers are comparable to those of the rotating-disc electrode at long distance [51]. These kinds of models are relatively easy to solve, but the model accuracy can be rather limited. However, recent development in both computer hardware and software has made more complex models accessible even on tabletop computers. For example, recently Vega Mercado *et al.* proposed a novel electrochemical methodology to determine the partition coefficient of neutral weak bases [53^{*}]. In this case, forced convection by a rotating rod in the top phase was used to enhance the mass transfer to and from the top phase, and the relationships between charges transferred during the forward sweep of the CV at different rotation rates and at different pHs allow determination of the partition coefficients of weak bases. Models of varying complexity were developed to validate the methodology, whereas magnetic resonance imaging (MRI, also sometimes called nuclear magnetic resonance (NMR) imaging) was utilized to experimentally validate the computational fluid dynamic (CFD) simulations, both in 2D and 3D. This article is an example of the complex combination of both CFD simulations with those of mass transfer in two phases, acid-base reactions, partitioning of neutral species, and potential controlled IT. The discrepancy between the simulated and experimental velocity values show that further development is still required especially for 3D modeling, but the trends are reproduced remarkably well, as shown in Figure 2.

Moving boundary model was utilized by Oseland *et al.* [54^{*}], who used a 1D FEM model to study amine (jefamine D230) transfer from an expanding droplet into an aqueous solution. Microelectrochemical measurements at expanding droplets were used to probe the potentiometric response of a pH sensitive microelectrode, and this response could be converted to give the concentration profile of the amine as a function of the electrode-

Figure 2

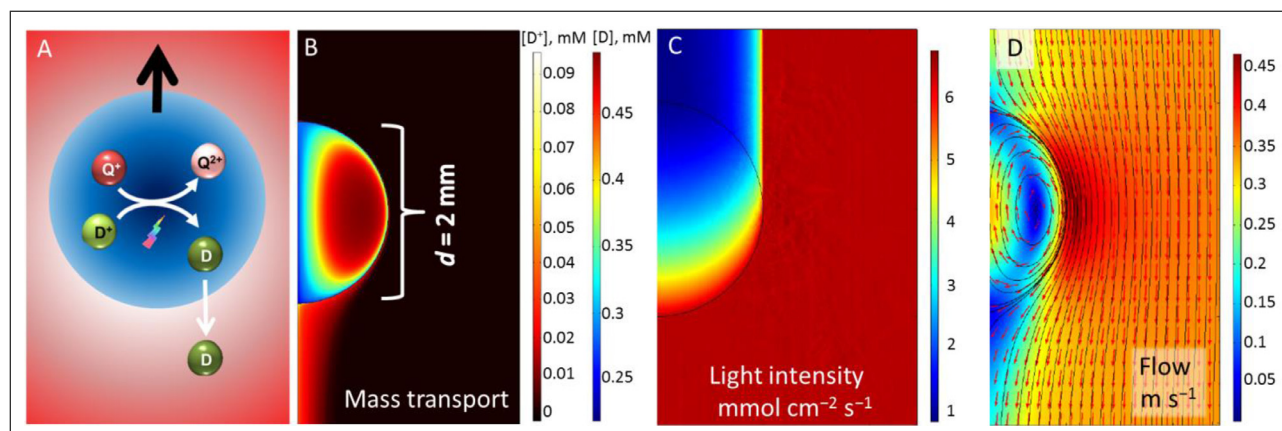


Comparison of the z-velocity maps obtained for the aqueous phase in a cylindrical cell, with a rotating rod ($r = 3$ mm) at $\omega = 62.8$ Hz from 3D FEM simulation of laminar flow (left) and from MRI, both in y, z-planes. ITIES is located at the bottom of the figure and there is negligible convection in the DCE phase. The asymmetry results from a slight misalignment between the rotating rod and the cell. Source: Adapted from Journal of Electroanalytical Chemistry, Vol 791, Vega Mercado F, Ovejero JM, Zanotto FM, Serial MR, Velasco MI, Fernández RA, Acosta RH, Dassie SA, Facilitated proton transfer across liquid|liquid interfaces under forced hydrodynamic conditions. Determination of partition coefficients of neutral weak bases, Pages No. 64-74, Copyright 2017, with permission from Elsevier [53^{*}].

droplet separation when the measurement was coupled with time-lapse microscopy. The theoretical concentration profile obtained with a moving plane model in COMSOL to describe the expanding droplet matched well the experimental data [54^{*}]. Moving boundaries are important for applications where shape and size of the droplet changes over time, for deposition of solids at LLI etc. and further development is expected to see these models utilized for understanding these effects better. For example, the shape of a droplet on an electrode depends on the applied potential, so digital simulations corroborated by experiments would be beneficial for understanding the electrochemical response upon droplet collision with an electrode.

Furthermore, a fundamental question that is still of importance is the adsorption of species at an ITIES and in the vicinity on the material walls of electrolytic cells. This has previously been explored by Méndez *et al.* [55] using a Guoy–Chapman model for species adsorbing at the interface, while Ellis *et al.* [56] examined species adsorbing on the pore wall of a micro-pore ITIES through a Langmuir

Figure 3



(A) Operating principle of the photo-ionic cell, where the dye is photoreduced in aqueous phase and extracted into the organic phase. (B) Digital simulations of mass transport; (C) absorption of light; and (D) fluid flow are required to estimate the system performance and to determine the critical parameters. Here an example of a 2 mm diameter droplet of aqueous phase containing 0.5 mM of the dye, moving up at the terminal velocity of 0.34 m/s in organic phase, under ca. 1 sun illumination from below. Simulations were done in 2D axis symmetric mode [58[•]]. Source: Adapted with permission from J. Phys. Chem. C, 119 (2015) 4728–4735. Copyright 2015 American Chemical Society [58[•]].

model. It would be interesting to combine these two perspectives as well as include other phenomena, like photocatalytic processes or the influence of adsorbed nanoparticles.

Photochemical charge transfer reactions

Another example of utilizing multiphysics digital simulations was demonstrated by Méndez *et al.* [57] for investigating photochemical reactions at LLIs under hydrodynamic convection in a system for conversion and storage of solar energy: photo-ionic cells. The solar energy is converted to chemical energy in a homogenous photochemical reaction between a sensitizer and a quencher, and stored by extraction of the photoproduct into the organic adjacent phase (as shown in Figure 3A), followed by physical separation of the phases. The energy can be recovered electrochemically with a biphasic fuel cell to produce electricity on demand [57]. Photochemical reactions have a large number of parameters affecting the quantum yield and efficiency of the system, so digital simulations are useful to pinpoint the most critical ones for further optimization. This requires coupling of simulations for both the light absorption and the mass transport of reactants, as well as computational fluid dynamics to account for the fluid flow; some results are illustrated in Figure 3B–D [58[•]]. The FEM simulations were used to evaluate the conditions required to reach large quantum yields of over 50%: long excited state lifetime (in the order of 10–100 μ s), large partition coefficient for the hydrophobic photoproduct, reasonable dye concentrations and large redox potential difference between the sensitizer and the quencher [57]. The simulations also show that the photoreaction should take place very close to the LLI to minimize the diffusion lengths and time to avoid

recombination reactions. Further simulations were performed to evaluate the effect of the droplet size on the attainable quantum yield [58[•]]. These papers give an example of utilizing digital simulations for “debottlenecking”, where the effect of the different parameters are evaluated to give guidelines about what is required to achieve high utilization of light.

Conclusions and perspectives

This review has shown that digital simulations have been utilized to analyze experimental results involving interfacial charge transfer reactions, moving interfaces, partition and complexation of species, photoreactions and forced hydrodynamic convection.

As computational power further increases and the requisite cost (in terms of both time and monetarily with regards to computational processing power and memory) becomes more affordable/achievable, the use of simulation software toward geometric, materials, etc., problems will become more ubiquitous and further exploit the ‘multi-physics’ aspect. That is to say, the inherent power of this method is not only to merge geometric and mass transport properties together, but is likely to expand to incorporate the interaction of other physical parameters, e.g., capacitance models, surface tension (e.g. through moving boundary), as well as nanoparticle interactions, etc., not to mention 3D aspects, pushing the frontier understanding and physical insight of complex processes of LLI systems.

As stated in the review by Arrigan and Herzog [8[•]] about miniaturized ITIES: “truly comprehensive models that incorporate mass transport, kinetics and capacitance, to

enable a complete characterization of a system under dynamic electrochemical conditions have yet to appear". This review indicates that significant progress has been made in comprehensive modeling, and this trend will continue. However, it should be stressed that certain care has to be taken with simulations, and verification against experimental and analytical solutions should always be performed.

Acknowledgments

This publication has emanated from research by M.D.S. supported by the European Research Council through a Starting Grant (agreement no. 716792) and in part by a research grant from Science Foundation Ireland (SFI) under grant number 13/SIRG/2137. T.J.S. is grateful to the European Commission for a MSCA Horizon 2020 grant, project# DLV-708814. P.P. is grateful for the financial support from the Swiss National Science Foundation, grant Ambizione Energy 160553.

References and recommended reading

Papers of particular interest, published within the period of review, have been highlighted as:

- Paper of special interest.
- Paper of outstanding interest.

1. Gavaghan DJ, Gillow K, Süli E: **Adaptive finite element methods in electrochemistry**. *Langmuir* 2006, **22**(25):10666–10682.
 2. Nann T, Heinze J: **Simulation in electrochemistry using the finite element method part 2: scanning electrochemical microscopy**. *Electrochim Acta* 2003, **48**(27):3975–3980.
 3. Nann T, Heinze J: **Simulation in electrochemistry using the finite element method: part 1: the algorithm**. *Electrochem Commun* 1999, **1**(7):289–294.
 4. Samec Z: **Dynamic electrochemistry at the interface between two immiscible electrolytes**. *Electrochim Acta* 2012, **84**:21–28.
 5. Peljo P, Girault HH: **Liquid/liquid interfaces, Electrochemistry at**. In: *Encyclopedia of Analytical Chemistry*. John Wiley & Sons, Ltd.; 2012.
 6. Girault H: **Electrochemistry at liquid–liquid interfaces**. In: Bard AJ, Zoski CG. *Electroanalytical Chemistry*. CRC Press; 2010:1–104.
 7. Liu S, Li Q, Shao Y: **Electrochemistry at micro- and nanoscopic liquid/liquid interfaces**. *Chem Soc Rev* 2011, **40**:2236–2253.
 8. Arrigan DWM, Herzog G: **Theory of electrochemistry at miniaturised interfaces between two immiscible electrolyte solutions**. *Curr Opin Electrochem* 2017, **1**(1):66–72.
- More detailed description of both experimental and theoretical progress for electrochemistry at miniaturised liquid|liquid interfaces.
9. Amemiya S, Wang Y, Mirkin MV: **Chapter 1: nanoelectrochemistry at the liquid/liquid interfaces**. In: *Electrochemistry: Volume 12*, 12. The Royal Society of Chemistry; 2014:1–43.
 10. Zanotto FM, Fernández RA, Dassie SA: **Theoretical model of ion transfer-electron transfer coupled reactions at the thick-film modified electrodes**. *J Electroanal Chem* 2017, **784**:25–32.
- Theory of coupling of ET-IT reactions at thick-film modified electrodes, how these two processes interrelate, particularly with respect to the resultant *i*-V signal.
11. Bobacka J, Ivaska A, Lewenstam A: **Potentiometric ion sensors**. *Chem Rev* 2008, **108**(2):329–351.
 12. Lewenstam A: **Non-equilibrium potentiometry—the very essence**. *J Solid State Electrochem* 2011, **15**(1):15–22.
 13. Ishimatsu R, Izadyar A, Kabagambe B, Kim Y, Kim J, Amemiya S: **Electrochemical mechanism of ion-ionophore recognition at plasticized polymer membrane/water interfaces**. *J Am Chem Soc* 2011, **133**(40):16300–16308.
 14. Garada MB, Kabagambe B, Amemiya S: **Extraction or adsorption? Voltammetric assessment of protamine transfer at ionophore-based polymeric membranes**. *Anal Chem* 2015, **87**(10):5348–5355.
 15. Yuan D, Cuartero M, Crespo GA, Bakker E: **Voltammetric thin-layer ionophore-based films: part 2. Semi-empirical treatment**. *Anal Chem* 2017, **89**(1):595–602.
- Model for thin-layer polymeric ionophore based films predict between two modes: diffusive mass transport or oxidation of the polymer. In this way, experimental conditions can be tuned to select for a desired ion at low concentrations (μM).
16. Yuan D, Cuartero M, Crespo GA, Bakker E: **Voltammetric thin-layer ionophore-based films: part 1. Experimental evidence and numerical simulations**. *Anal Chem* 2017, **89**(1):586–594.
 17. Liu C, Peljo P, Huang X, Cheng W, Wang L, Deng H: **Single organic droplet collision voltammogram via electron transfer coupled ion transfer**. *Anal Chem* 2017, **89**(17):9284–9291.
- Simulations of single emulsion soft matter particle (femtolitre) impacts at a solid electrode which predict the particle angle upon impact as well as the *i*R drop in the oil phase, which was shown to be negligible.
18. Peljo P, Smirnov E, Girault HH: **Heterogeneous versus homogeneous electron transfer reactions at liquid–liquid interfaces: the wrong question?** *J Electroanal Chem* 2016, **779**:187–198.
- Interrogation of the ET mechanism of the Fc/Fe(CN)₆⁴⁻ across a LLI showed that it occurs as a bulk process in the w phase with the observed current originating from the IT of the oxidised Fc⁺ product. If a nanofilm is introduced, it behaves as a bipolar electrode and the mechanism ET becomes heterogeneous.
19. Hotta H, Ichikawa S, Sugihara T, Osakai T: **Clarification of the mechanism of interfacial electron-transfer reaction between ferrocene and hexacyanoferrate (iii) by digital simulation of cyclic voltammograms**. *J Phys Chem B* 2003, **107**(36):9717–9725.
 20. Peljo P, Scanlon MD, Olaya AJ, Rivier L, Smirnov E, Girault HH: **Redox electrocatalysis of floating nanoparticles: determining electrocatalytic properties without the influence of solid supports**. *J Phys Chem Lett* 2017, **8**(15):3564–3575.
 21. Stockmann TJ, Angelé L, Brasiense V, Combellas C, Kanoufi F: **Platinum nanoparticle impacts at a liquid|liquid interface**. *Angew Chem Int Ed* 2017. <https://doi.org/10.1002/anie.201707589>.
- Single nanoparticle detection through catalytic enhancement via Pt nanoparticle catalyzed O₂ reduction. Simulations explore nanoparticle penetration across the ITIES.
22. Trojánek A, Langmaier J, Samec Z: **Electrocatalysis of the oxygen reduction at a polarised interface between two immiscible electrolyte solutions by electrochemically generated Pt particles**. *Electrochem Commun* 2006, **8**(3):475–481.
 23. Momotenko D, Pereira CM, Girault HH: **Differential capacitance of liquid/liquid interfaces of finite thicknesses: a finite element study**. *Phys Chem Chem Phys* 2012, **14**(32):11268–11272.
 24. Gschwend GC, Smirnov E, Peljo P, Girault H: **Electrovariable gold nanoparticle films at liquid-liquid interfaces: from redox electrocatalysis to marangoni-shutters**. *Faraday Discuss* 2017, **199**:565–583.
 25. Deryabina MA, Hansen SH, Jensen H: **Versatile flow-injection amperometric ion detector based on an interface between two immiscible electrolyte solutions: numerical and experimental characterization**. *Anal Chem* 2011, **83**(19):7388–7393.
 26. Rivier L, Stockmann TJ, Méndez MA, Scanlon MD, Peljo P, Opallo M, Girault HH: **Decamethylruthenocene hydride and hydrogen formation at liquid|liquid interfaces**. *J Phys Chem C* 2015, **119**(46):25761–25769.
- Example of utilising digital simulations for understanding electrocatalytic reactions at liquid–liquid interfaces.
27. Stockmann TJ, Deng H, Peljo P, Kontturi K, Opallo M, Girault HH: **Mechanism of oxygen reduction by metallocenes near liquid|liquid interfaces**. *J Electroanal Chem* 2014, **729**:43–52.

28. Deng H, Stockmann TJ, Peljo P, Opallo M, Girault HH: **Electrochemical oxygen reduction at soft interfaces catalyzed by the transfer of hydrated lithium cations.** *J Electroanal Chem* 2014, **731**:28–35.
29. Deng H, Peljo P, Stockmann TJ, Qiao L, Vainikka T, Kontturi K, Opallo M, Girault HH: **Surprising acidity of hydrated lithium cations in organic solvents.** *Chem Commun* 2014, **50**(42):5554–5557.
30. Wightman RM: **Microvoltammetric electrodes.** *Anal Chem* 1981, **53**(9):1125A–1134A.
31. Taylor G, Girault HHJ: **Ion transfer reactions across a liquid–liquid interface supported on a micropipette tip.** *J Electroanal Chem* 1986, **208**(1):179–183.
32. Arrigan DWM, Liu Y: **Electroanalytical ventures at nanoscale interfaces between immiscible liquids.** *Annu Rev Anal Chem* 2016, **9**(1):145–161.
33. Mirkin M: **Nanoelectrodes and liquid/liquid nanointerfaces.** *Nanoelectrochemistry*. CRC Press; 2015:539–572.
34. Jossierand J, Morandini J, Lee HJ, Ferrigno R, Girault HH: **Finite element simulation of ion transfer reactions at a single micro-liquid|liquid interface supported on a thin polymer film.** *J Electroanal Chem* 1999, **468**(1):42–52.
35. Strutwolf J, Arrigan DWM: **Optimisation of the conditions for stripping voltammetric analysis at liquid–liquid interfaces supported at micropore arrays: a computational simulation.** *Anal Bioanal Chem* 2010, **398**(4):1625–1631.
36. Strutwolf J, Scanlon MD, Arrigan DWM: **Electrochemical ion transfer across liquid/liquid interfaces confined within solid-state micropore arrays - simulations and experiments.** *Analyst* 2009, **134**(1):148–158.
37. Nishi N, Imakura S, Kakiuchi T: **A digital simulation study of steady-state voltammograms for the ion transfer across the liquid–liquid interface formed at the orifice of a micropipette.** *J Electroanal Chem* 2008, **621**(2):297–303.
38. Rodgers PJ, Amemiya S, Wang Y, Mirkin MV: **Nanopipet voltammetry of common ions across the liquid–liquid interface. Theory and limitations in kinetic analysis of nanoelectrode voltammograms.** *Anal Chem* 2009, **82**(1):84–90.
39. Alvarez de Eulate E, Strutwolf J, Liu Y, O'Donnell K, Arrigan DWM: **An electrochemical sensing platform based on liquid–liquid microinterface arrays formed in laser-ablated glass membranes.** *Anal Chem* 2016, **88**(5):2596–2604.
40. Nishi N, Murakami H, Imakura S, Kakiuchi T: **Facilitated transfer of alkali-metal cations by dibenzo-18-crown-6 across the electrochemically polarized interface between an aqueous solution and a hydrophobic room-temperature ionic liquid.** *Anal Chem* 2006, **78**(16):5805–5812.
41. Stockmann TJ, Noel J-M, Abou-Hassan A, Combellas C, Kanoufi F: **Facilitated lewis acid transfer by phospholipids at a (water|CHCl₃) liquid|liquid interface towards biomimetic and energy applications.** *J Phys Chem C* 2016, **120**(22):11977–11983.
42. Adamiak W, Jedraszko J, Nogala W, Jönsson-Niedziolka M, Dongmo S, Wittstock G, Girault HH, Opallo M: **A simple liquid–liquid biphasic system for hydrogen peroxide generation.** *J Phys Chem C* 2015, **119**(34):20011–20015.
43. Wang Y, Kececi K, Velmurugan J, Mirkin MV: **Electron transfer/ion transfer mode of scanning electrochemical microscopy (SECM): a new tool for imaging and kinetic studies.** *Chem Sci* 2013, **4**(9):3606–3616.
44. Zhou M, Yu Y, Hu K, Mirkin MV: **Nanoelectrochemical approach to detecting short-lived intermediates of electrocatalytic oxygen reduction.** *J Am Chem Soc* 2015, **137**(20):6517–6523.
45. Oleinick A, Yu Y, Svir I, Mirkin MV, Amatore C: **Theory and simulations for the electron-transfer/ion-transfer mode of scanning electrochemical microscopy in the presence or absence of homogenous kinetics.** *ChemElectroChem* 2017, **4**(2):287–295.
- ET/IT mode of SECM is elucidated for the investigation of heterogeneous substrate reactions, with charged products.
46. Deng H, Peljo P, Momotenko D, Cortés-Salazar F, Stockmann TJ, Kontturi K, Opallo M, Girault HH: **Kinetic differentiation of bulk/interfacial oxygen reduction mechanisms at/near liquid/liquid interfaces using scanning electrochemical microscopy.** *J Electroanal Chem* 2014, **732**:101–109.
47. Shen M, Ishimatsu R, Kim J, Amemiya S: **Quantitative imaging of ion transport through single nanopores by high-resolution scanning electrochemical microscopy.** *J Am Chem Soc* 2012, **134**(24):9856–9859.
48. Chen R, Balla RJ, Lima A, Amemiya S: **Characterization of nanopipet-supported ITIES tips for scanning electrochemical microscopy of single solid-state nanopores.** *Anal Chem* 2017, **89**(18):9946–9952.
49. Kuss S, Trinh D, Mauzeroll J: **High-speed scanning electrochemical microscopy method for substrate kinetic determination: application to live cell imaging in human cancer.** *Anal Chem* 2015, **87**(16):8102–8106.
50. Henderson JD, Filice FP, Li MSM, Ding Z: **Tracking live-cell response to hexavalent chromium toxicity by using scanning electrochemical microscopy.** *ChemElectroChem* 2017, **4**(4):856–863.
51. Ovejero JM, Fernández RA, Dassie SA: **Ion transfer across liquid|liquid interface under forced hydrodynamic conditions. I: digital simulations.** *J Electroanal Chem* 2012, **666**:42–51.
52. Levich VG: *Physicochemical Hydrodynamics*. Englewood Cliffs (NJ): Prentice-Hall; 1962.
53. Vega Mercado F, Ovejero JM, Zanotto FM, Serial MR, Velasco MI, Fernández RA, Acosta RH, Dassie SA: **Facilitated proton transfer across liquid|liquid interfaces under forced hydrodynamic conditions. Determination of partition coefficients of neutral weak bases.** *J Electroanal Chem* 2017, **791**:64–74.
- Partitioning of neutral bases at a macro w|o interface under forced hydrodynamic conditions is modelled and correlated by multiple analytical techniques.
54. Oseland EE, Rea A, de Heer MI, Fowler JD, Unwin PR: **Interfacial kinetics in a model emulsion polymerisation system using microelectrochemical measurements at expanding droplets (MEMED) and time lapse microscopy.** *J Colloid Interface Sci* 2017, **490**:703–709.
- Partition of an amine is investigated at an expanding oil–water droplet using a microelectrode and modelled with a moving boundary.
55. Méndez MA, Su B, Girault HH: **Voltammetry for surface-active ions at polarisable liquid|liquid interfaces.** *J Electroanal Chem* 2009, **634**(2):82–89.
56. Ellis JS, Strutwolf J, Arrigan DWM: **Finite-element simulations of the influence of pore wall adsorption on cyclic voltammetry of ion transfer across a liquid–liquid interface formed at a micropore.** *Phys Chem Chem Phys* 2012, **14**:2494–2500.
57. Méndez MA, Peljo P, Scanlon MD, Vrabel H, Girault HH: **Photo-ionic cells: two solutions to store solar energy and generate electricity on demand.** *J Phys Chem C* 2014, **118**(30):16872–16883.
58. Bourdon R, Peljo P, Méndez MA, Olaya AJ, De Jonghe-Risse J, Vrabel H, Girault HH: **Chaotropic agents boosting the performance of photoionic cells.** *J Phys Chem C* 2015, **119**(9):4728–4735.
- Example of simulations of mass transfer, light adsorption and photoreactions, and hydrodynamics for evaluation of the system performance.